MR Imaging of Knee Implants Using SEMAC at 3T

TAO AI[1], Panli Zuo[2], Yiqi Hu[1], Mathias Nittka[3], and Liming Xia[1]

[1]*Radiology, Tongji Hospital, Tongji Medical College, Huazhong University of Science and Technology, Wuhan, Hubei, China,* [2]*Siemens Healthcare, MR Collaborations NE Asia, Beijing, China,* [3]*Siemens Healthcare, Germany, Erlangen, Germany*

Target audience

Most radiologists, orthopedic surgeons and some medical physicists who are working on MR imaging will benefit from this information out of this study.

Purpose

Since SEMAC has been successfully implemented at 1.5T in various clinical applications of different human body parts with different metal implants, little has been reported about applications at higher field strength. Thus we designed this study to investigate the efficacy of SEMAC and high bandwidth (high BW) techniques in metal artifact reduction and clinical applications at 3T MR imaging.

Materials and Methods

Fig. 1

Two sets of total knee replacements (Cobalt Chromium/Titanium [CoCr/Ti] and Oxidized Zirconium/ Titanium [OxZr/Ti]) were surgically fixed into bovine knees to make two tissue-based phantoms. Small holes were drilled and four plastic tubes filled with gadolinium doped agarose gel (measuring 25 mm in length and 3.5 mm in diameter) were inserted into the medial and lateral femoral condyles, two in each, with one end of each tube contacting the metal component of the implant in all cases. The other two tubes were placed into the medial and lateral tibial plateaus with the end against tibial metal component **(Fig. 1)**. Both tissue specimens were scanned at 3T (MAGNETOM Skyra, Siemens Healthcare) equipped with a 15-channel knee coil, using a prototype SEMAC sequence (15 SEMAC-encoding steps) with high readout bandwidth (high BW, BW=501Hz/pixel) and a product TSE sequence (BW= 241Hz/pixel); imaging included four contrasts: T1w, T2w, PDw and STIR. In addition, 11 knees with total implants in ten patients were scanned using the same imaging protocols. Quantitative analysis was done in two tissue specimens by measuring the visible length (L_{normal}) of the gadolinium-filled tubes, which was taken at the same slice location for different imaging sequences. In this way, the extent of the metal artifact involved ($L_{artifact}$) can be calculated by the equation ($L_{artifact}$ = 25mm - L_{normal}), in other words we can quantify, how closely we can evaluate the normal tissues or implant-related complications adjacent to the metal implants. In addition, qualitative analysis was performed in both tissue specimens and human scans by blinded readers, with regard to the artifact size, distortion, and image quality based on the anatomic segments.

Fig. 2

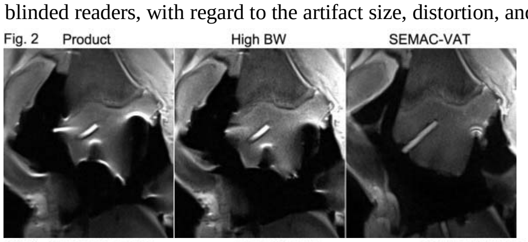

Results and Discussion

For quantitative measurements, the length of visible normal tube (L_{normal}) adjacent to femoral CoCr component was 8.0±1.2mm, 9.6±1.1mm and 22.7±1.5mm for product, high BW and SEMAC; the tube length adjacent to the femoral OxZr component was 17.5±1.6mm, 18.9±1.7mm and 22.6±0.6mm, respectively. The difference was statistically significant among the three imaging techniques for both types of metal components. These results demonstrated that the SEMAC-technique significantly improved the visualization of tissue structures adjacent to the metal implants, in particular with OxZr/Ti components.

Fig. 3

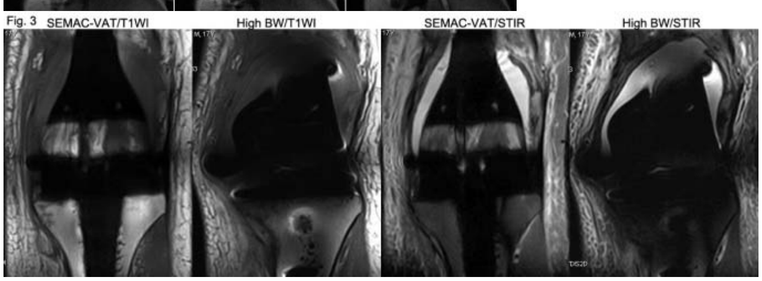

The tube length adjacent to the tibial Ti component was 9.2±0.4mm (CoCr/Ti) and 23.3±0.4mm (OxZr/Ti) with product; 15.8±0.3mm (CoCr/Ti) and 23.2±0.4mm (OxZr/Ti) with high BW; 23.1±0.8mm (CoCr/Ti) and 23.2±0.5mm (OxZr/Ti) with SEMAC **(Fig. 2)**. There was a significant difference in visible tube length for the CoCr/Ti implant among all three sequence techniques; however, no significant difference was observed with OxZr/Ti implant (which has better physical properties for in vivo MR imaging). These results indicate that the artifact extended from the femoral metallic component would significantly obscure the interface between the Ti component and tibial plateau, in particular with the CoCr/Ti implant, which can be improved by using SEMAC. For qualitative evaluation of tissue specimen and human knees with metallic implants, the scoring results are presented as mean±standard deviation (SD) in **Table 1**. The metal-related artifact size, distortion of tissue structures adjacent to metal implants, and the overall image quality and diagnostic confidence were significantly improved by using the SEMAC technique as compared to the high bandwidth and the conventional product sequence. For human knee scans, the scores of MR images with SEMAC were 1.62±0.21, 1.48±0.39, and 2.25±0.72 for artifact size, distortion and image quality, as compared with the conventional sequence (2.79±0.33, 2.82±0.54 and 0.87±0.62 respectively). The differences were statistically significant (all $P<0.05$). However, the image contrast and the details of tissue structures were compromised because of lower flip angle used with SEMAC (due to SAR limitations). In addition, each sequence combined with SEMAC would take 6 to 8 minutes (even longer in STIR), which makes it impossible to implement SEMAC into the every scanning protocols by now. Thus more optimizations should be made in future to shorten acquisition time and improve image quality at 3T.

Table 1. The scoring results of tissue specimens with different metal implants and sequence variants by blinded reads, using a 4-point scale.

		SEMAC	High BW	Product
Artifact Size	OxZr	1.65±0.28*	2.75±0.27	2.85±0.20
	CoCr	1.33±0.32*	2.38±0.34*	2.88±0.26
Distortion	OxZr	1.48±0.26*	2.50±0.35	2.73±0.31
	CoCr	1.30±0.38*	2.45±0.29*	2.88±0.26
Image Quality and	OxZr	2.38±0.86*	1.00±0.71	0.75±0.43
Diagnostic Confidence	CoCr	2.38±0.70*	1.25±0.43*	0.50±1.00

*P-value < 0.05, as compared with Product sequence.

Conclusions

SEMAC allows for significant metal artifact reduction and distortion correction at 3T MR imaging of knee implants, as compared with the conventional and increased readout bandwidth sequences. With optimizations, SEMAC would be routinely chosen for the clinical application of knee prosthesis.

References

[1] Ai T, et al. *Invest Radiol. 2012 May;47(5):267-76.*[2] Sutter R, et al. *AJR Am J Roentgenol. 2013 Dec;201(6):1315-24.* [3] Bachschmidt TJ, et al. *J Magn Reson Imaging. 2014 Aug 23.*